Journal of Engineering and Applied Sciences 2 (11): 1669-1676, 2007
ISSN: 1816-949X

Structural Analysis of Corroded Deck Plating of a Work Barge in Marine Operations

A.U. Ibekwe, I.E. Douglas and S. Odi-Owei
Rivers State University of Science and Technology,
P.M.B 5080, Port Harcourt, Nigeria

Abstract: Marine crafts operating in the Niger Delta regions of Nigeria experience exceptionally high level of corrosion due to the high water salinity, humidity and acidic effluents from oil and gas operations. This most often results in rapid and serious pitting (of the hull plating and other steel members) that weaken the hull structural assemblage. This study presents a finite element methodology of evaluating the structural integrity of pitted hull plating. The approach is based on a statistical derivation of thickness variations due to pitting. A primary input to the analysis is the definition of the pitting profile consistent with classification societies' categorization. The main functional components of a visual basic code developed to implement the finite element formulation are described. Results of the analyses are discussed and presented in graphical and tabular forms.

Key words: Structural analysis, corroded deck plating, marine work barge, variable thickness, modelling

INTRODUCTION

The importance of plates as slabs in decks, platform floors, containment structures, as well as in walls and bulkheads cannot be overstated. Plates in service operate under a variety of loading and boundary conditions and as such should satisfy not only its functional requirements, but structurally withstand these conditions in service to avoid or reduce the social and economic consequences of failure.

A predominant characteristic of the deltaic areas of Nigeria is the high corrosivity of its environment. The high salinity of the sea, acid rain combined with crude oil activities present serious corrosion problems to ferrous materials used in the construction of marine crafts operating in the region (Climate Justice, 2005; Akpan, 2003). It is indeed common to observe exposed steel pipes, gratings, etc corrode with abnormal rapidity. Another significant effect is the corrosion of ship hull and deck plating to varying degrees, especially for vessels that have been in service for extended periods.

The primary effect on steel corrosion in a crude oil/brine environment is apparently on the protectiveness of the corrosion product layer formed on the steel and with adverse weather conditions such as heavy rainfall, the protective coatings are soon eroded to expose surface for attacks. Crevices (pits) formed; provide boundaries for accelerated attack through Environmentally Assisted Crack Growth (EACG) (Corrosion Doctor, 2007) under cyclic or sustained loading conditions, by the creation of a damaged state not envisioned in the structural damage or fatigue analysis.

Surface metal losses due to corrosion among other reasons result in a variable thickness profile (Lakhote *et al*., 2002) which has been modelled by the two-dimensional Fourier series (Roorda *et al*., 1996). This creates a prebuckling stress field, which has a significant influence on displacement, associated stresses and buckling load and as such, their assessment in service, resulting in a better prediction of the structural integrity of corroded plates is considered a problem of practical importance (Johnary, 2005).

The importance of thickness reduction in structural members especially due to corrosion is further elucidated in a Classification Society's categorization for thickness acceptance criteria (BVMD, 2000) which stipulates the limits of metal wastage to be allowed for reinforcements, repairs, or renewal of steel structures. The acceptance criterion is generally based among others, on the pitting conditions of the structural members relative to the as-built thickness. The randomness of the pits distribution has thus been modeled by a statistical approach using least squares method to fit a 3rd degree polynomial to obtain an approximate correlation used in deriving a discretization pattern for the finite element analysis of the corroded deck plating (Ibekwe, 2006).

The finite element modelling using this novel concept of statistically derived thickness profile of the corroded plate considers the structure as an assemblage of all individual triangular elements following a well defined

Corresponding Author: I.E. Douglas, Rivers State University of Science and Technology, PMB 5080, Port Harcourt, Nigeria

procedure of establishing local equilibrium at each node. The functionalities of the concept was thus incorporated in developing an algorithm in Visual Basic, an object oriented, graphic user interface based programming language, which declares parameters and codes that define function procedures as names and having the added advantage of ease of access and procedure modifiers.

Validation of the Finite Element Visual Basic algorithm was carried out by a comparative analysis which showed an error margin of 1.031% to results obtained from classical formulations for a uniform loaded encastre plate of 1.1 aspect ratio (Timoshenko and Woinowsky, 1959). The program is however limited to rectangular plates built in on all sides, employing triangular elements only.

Theoretical formulation: Arbitrary thickness variation for reasons of geometrical non-linearity largely due to surface losses from corrosion, with plate material properties remaining homogenous, can result in the variation of plate flexural rigidity whose value is largely dependent on the value of thickness t, at any point on the plate surface. The stochastic and complex discontinuous boundaries make such problems difficult or impossible to describe mathematically.

However, a novel analytical technique has been adapted from the Finite Element method, to model the overall structural stiffness of the plate. The method of Finite Element (FEM), which is a general numerical procedure for the approximate analysis of arbitrary structural systems and a powerful tool in the evaluation of new designs with respect to offshore structures with the problem of load, strength and foundation analysis handled to a satisfactory level of confidence (Sletten and Pederson, 1974), has been extensively developed and published (Rockey *et al*., 1973; Zienkiewicz, 1971; Clough *et al*., 1956; Ross, 1982). A simple numerical concept employing the method of least squares to fit an n-degree polynomial from measured thickness data for an arbitrarily corroding plate, along its discretized rows or columns to obtain an equivalent element thickness, t_e and consequently, an overall structural stiffness of the plate continuum has been recently considered and incorporated to develop a computational software based on the Finite Element analysis (Ibekwe, 2006).

The key to the method is the general matrix linear equation relating elemental load to their corresponding nodal displacements given as

$$\{F^e\} = [K^e]\{\partial^e\} \quad (1)$$

A partitioned method of matrix summation of the contributions of all element stiffness matrices results in

$$\{F\} = [K]\{\partial\} \quad (2)$$

The overall stiffness matrix [K] relates the applied nodal forces to the unknown displacement, upon which the displacement vector for the entire structure can be determined for any given load, after consideration of the given boundary conditions.

In general matrix form, the algebraic equation from which a unique curve for each discretized row or column is fitted to obtain nodal thicknesses for a given set of measured data points (x_i,y_i), by application of least square errors;

Square errors (e^2) expressed as

$$e^2 = \sum_{t=1}^{m}\left(t_i - a_0 - a_{1i}t_i - a_{2i}t_i^{\,2} - a_{3i}t_i^{\,3} - - - - - - a_{ni}t_i^{\,n}\right)^2 = f(t) \quad (3)$$

Minimizing the square errors (i.e. least square errors) gives

$$\frac{\partial f(t)}{\partial a_i} = 0$$

which yields the following in the expanded matrix form:

$$\begin{bmatrix} n & \sum x_i & \sum x_i^2 & \sum x_i^3 & . & . & \sum x_i^n \\ \sum x_i & \sum x_i^2 & \sum x_i^3 & \sum x_i^4 & . & . & \sum x_i^{n+1} \\ \sum x_i^2 & \sum x_i^3 & \sum x_i^4 & . & . & . & \sum x_i^{n+2} \\ \sum x_i^3 & \sum x_i^4 & \sum x_i^5 & . & . & . & \sum x_i^{n+3} \\ . & . & . & . & . & . & . \\ . & . & . & . & . & . & . \\ \sum x_i^n & \sum x_i^{n+1} & \sum x_i^{n+2} & \sum x_i^{n+3} & . & . & \sum x_i^{2n} \end{bmatrix} \cdot \begin{bmatrix} a_0 \\ a_1 \\ a_2 \\ a_3 \\ . \\ . \\ a_n \end{bmatrix} = \begin{bmatrix} \sum t_i \\ \sum t_i x_i \\ \sum t_i x_i^2 \\ \sum t_i x_i^3 \\ . \\ . \\ \sum t_i x_i^n \end{bmatrix} \quad (4)$$

Such that

$$f(x_1) = t_1,\ f(x_2) = t_2, \ldots\ldots\ldots\ldots\ldots, f(x_{n-1}) = t_{n-1},\ f(x_n) = t_n$$

along the transverse or longitudinal axes.

In addition, as the Finite Element theory is defined for constant cross section, an equivalent element thickness, t_e is obtained as a simple average of its boundary nodal thickness as

$$t_e = \frac{1}{3}\sum_{i=1}^{3} t_{node\ i} \quad (5)$$

The Finite Element algorithm from first principle for a triangular element has been adapted in developing a visual basic program to model the problem of plate flexure for an arbitrarily varying thickness profile due largely to corrosion and a comparative analysis of the results obtained from the software for a uniformly loaded encastre plate of 1.1 aspect ratio to those from classical formulations show an error margin of 1.031%.

MODEL APPLICATION TECHNIQUE

With the reasonable validation of the developed Finite Element software, the code was then extended to the stress analysis of the deck plate of a self-propelled rectangular work barge. A close up view showing the extent of plate corrosion in service as obtained from a condition survey report is as shown in Plate 1.

Barge geometry is presented in the structural details (Appendix I) and a corrosion pattern typical of the one shown in Plate 1 was used as general data for the analysis. Deck materials are made from Marine Grade (A) steels as stipulated by the general requirements for hot-rolled plates for use in ship construction and other marine structures (Lloyd's Register, 1997).

In performing the isolated analysis of deck panels, complete fixity by welding was assumed. Deck loads in the form of machinery and cargo were assigned as patch loads acting over a small area, to avoid the singularities associated with point actions of load, to three separate panels of sizes 2.5 m × 5.5 m (panel A), 3.5 m × 5.5 m (panel B) and 5.0 m × 5.5 m (panel C) for the 10 mm uniform thickness deck plate. Their responses were compared side by side to those observed for the same load conditions as the individual panels corrode to varying degrees.

In the three panels analyzed, arbitrary thickness gauging from which a 3rd degree polynomial curve was fitted for each longitudinal axis of the finite element discretization and individual element thicknesses determined in line with the pattern established for node numbering. In the simulation process, thickness losses due to pitting was varied approximately as 25, 45% and to a very severe case of 55% of the original uncorroded plate thickness, t_0.

Plate 1: Typical deck plate condition for a work barge in service

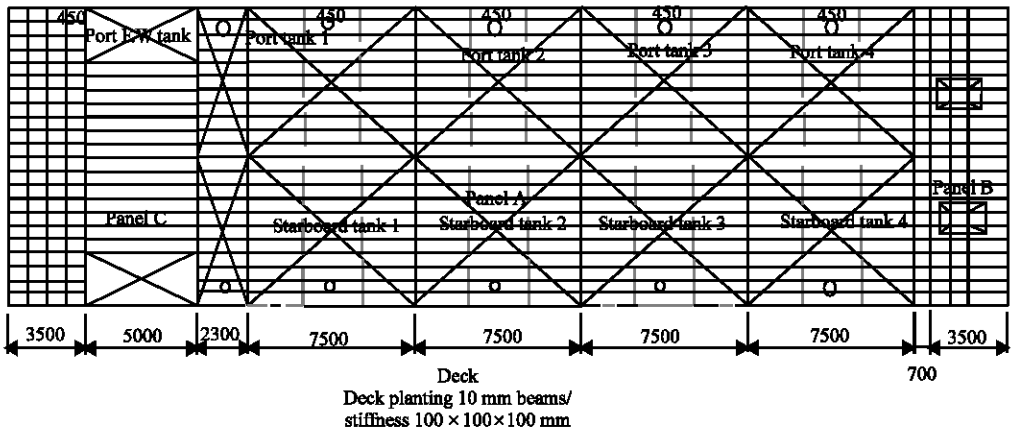

Appendix 1: Barge structural detail

RESULTS AND DISCUSSION

A comparison of the deflections (θ_x, θ_y, w) and reactions in the form of bending stresses (M_x, M_y, M_{xy}) for the panels analyzed for uniform thickness and those obtained for the various pitting levels for the same load conditions are presented in tables and charts. The critical points include the responses at their centre nodes, along the central longitudinal axes and along the central transverse axes. The isolated analyses of two individual panels are presented for brevity.

Analysis of the 25% pitted plate (Panel a): Panel A is typical of any of the 2.5×5.5 m deck plates, port or starboard of the amidships section. Optimal discretization employed a total of 189 nodes, starting from node 1-9 along the horizontal facing aft. For the loading considered, lateral displacement at the centre (node 95) had a value of 5.27 mm, while a maximum deflection of 5.361 mm occurred on node 104. The maximum x-moment occurring at node 6 had a value of 0.085KNm, while its minimum value of -0.117 occurred on node 185. Comparatively, the central nodal displacement in the 25% pitted case gave a higher value of 12.492 mm. Correspondingly, the maximum deflection obtained as 12.708 mm occurred on node 104. Maximum and minimum deflections about × in the pitted case occurred at the same nodal positions having values of 0.011rad and -0.007rad, respectively. A summary of variations of the other critical parameters is shown in Table 1 and 2.

Panel A Centreline longitudinal (along nodes 91-99) and transverse (along nodes 5-185) deflection profiles showing the responses for the cases of uniform thickness and thickness loss due to pitting are shown below in Fig. 1-3 and 4-6, respectively.

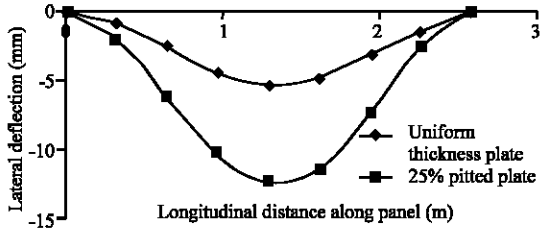

Fig. 1: Longitudinal lateral deflection profile

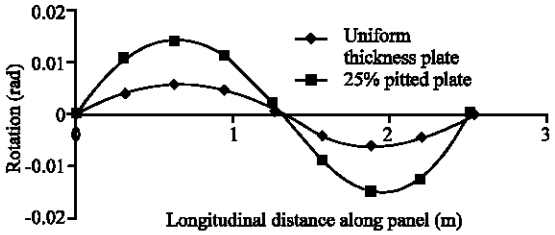

Fig. 2: Longitudinal angular deflection profile about x

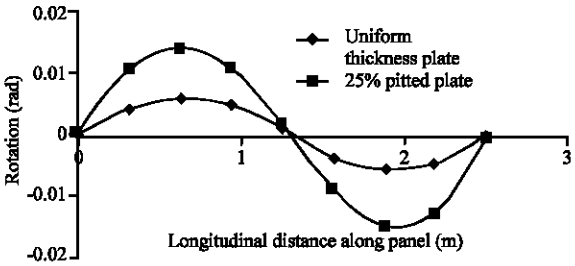

Fig. 3: Longitudinal angular deflection profile about y

Analysis of the 55% pitted plate (Panel c): The 5.0 m × 5.5 m aft deck plate representing Panel C was assumed to have reached an extreme case of thickness loss from

Table 1: Summary of critical response parameters for panel a

Node No.		Deflection											
Transv.	Long.	θ_x(rad)		θ_x^*(rad)		θ_y(rad)		θ_y^*(rad)		w(mm)		w*(mm)	
5	91	0	0	0	0	0	0	0	0	0	0	0	0
14	92	-0.003	0	-0.006	0	0	0.004	0	0.011	-0.455	-0.819	-1.077	-1.941
23	93	-0.003	0	-0.007	-0.001	0	0.006	0	0.014	-1.278	-2.564	-3.029	-6.077
32	94	-0.003	-0.001	-0.006	-0.002	0.001	0.005	-0.001	0.011	-2.078	-4.342	-4.925	-10.291
41	95	-0.002	-0.001	-0.005	-0.002	0	0.001	-0.001	0.002	-2.729	-5.270	-6.469	-12.492
50	96	-0.001	-0.001	-0.003	-0.002	0	-0.004	-0.001	-0.009	-3.185	-4.801	-7.548	-11.379
59	97	-0.001	-0.001	-0.003	-0.001	0	-0.006	0	-0.015	-3.504	-3.095	-8.306	-7.336
68	98	-0.001	0	-0.003	-0.001	0	-0.005	0.001	-0.013	-3.826	-1.052	-9.069	-2.494
77	99	-0.002	0	-0.004	0	0	0	0.001	0	-4.269	0	-10.118	0
86		-0.002		-0.004		0.001		0.002		-4.825		-11.436	
95		-0.001		-0.002		0.001		0.002		-5.270		-12.492	
104		0		0.001		0		0.002		-5.361		-12.708	
113		0.001		0.003		0		0.001		-5.097		-12.08	
122		0.001		0.003		0		0		-4.723		-11.193	
131		0.001		0.001		0		-0.001		-4.478		-10.614	
140		0.001		0.002		-0.001		-0.002		-4.324		-10.250	
149		0.002		0.005		-0.001		-0.002		-3.979		-9.430	
158		0.004		0.009		-0.001		-0.001		-3.181		-7.540	
167		0.005		0.011		0		-0.001		-1.936		-4.589	
176		0.004		0.009		0		0		-0.648		-1.535	
185		0		0		0		0		0		0	

*indicate values for the pitted case

Table 2: Maximum values of critical parameters for panel a

Node No.	Response parameter	Max. value
167	θ_x(rad)	0.005
167	θ_x^*(rad)	0.011
102	θ_y(rad)	0.006
102	θ_y^*(rad)	0.014
104	w(mm)	5.361
104	w*(mm)	12.708
6	M_x(KNm)	0.085
6	M_x^*(KNm)	0.085
99	M_y(KNm)	0.128
99	M_y^*(KNm)	0.128

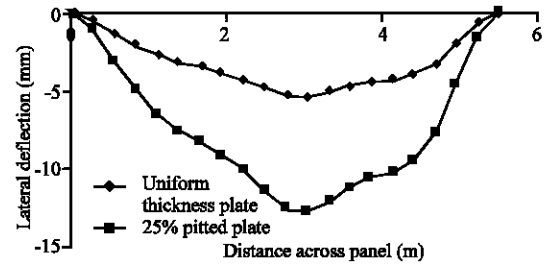

Fig. 4: Transverse lateral deflection profile

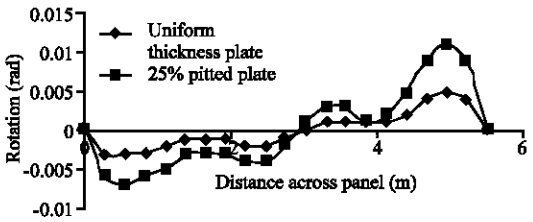

Fig. 5: Transverse angular deflection profile about x

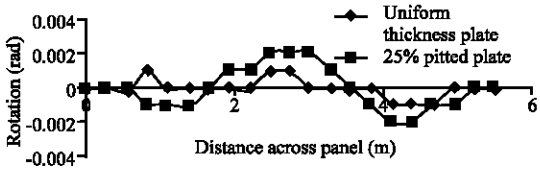

Fig. 6: Transverse angular deflection profile about y

severe pitting. The discretized section employing 441 nodes gave the maximum deflection value for the loading considered as 533.465 mm on the central node 221 for the pitted case, representing an outrageous 997.35% increase over the maximum deflection for the uncorroded plate for the same section. Reactions in both cases however showed nearly insignificant variations as pitting progressed. Table 3 and 4 show a summary of these critical responses. Similar plots of structural responses as in previous panels are shown in Fig. 7-12.

In general, lateral deflections in both the longitudinal and transverse axes as observed in all panels considered consistently showed significant increases for the pitted cases over those of the new ship (i.e. uncorroded deck plate). Progressive increases in deflection were similarly observed as the pitting level increased, the worst case being that of the 55% pitted panel. The rotations about x showed a similar trend in variation as the lateral deflections along both axes for small changes in thickness. Contrary to expectations

Table 3: Summary of critical response parameters for panel c

Node No.		Deflection											
Transv.	Long.	θ_x(rad)		θ_x^*(rad)		θ_y(rad)		θ_y^*(rad)		w(mm)		w*(mm)	
11	211	0	0	0	0	0	0	0	0	0	0	0	0
32	212	-0.003	0	-0.139	-0	0	0.013	0	0.139	-1.918	-1.714	-21.040	-18.803
53	213	-0.021	-0.001	-0.231	-0.01	0	0.021	0.003	0.234	-6.715	-6.092	-73.678	-66.850
74	214	-0.026	-0.001	-0.280	-0.01	0.001	0.026	0.006	0.289	-13.260	-12.160	-145.460	-133.480
95	215	-0.027	-0.001	-0.293	-0.02	-0.001	0.028	-0.014	0.312	-20.590	-19.120	-225.890	-209.750
116	216	-0.026	-0.001	-0.288	-0.01	0.001	0.028	0.009	0.311	-28.050	-26.300	-307.820	-288.570
137	217	-0.023	-0.001	-0.255	-0.01	0.001	0.026	0.008	0.287	-34.970	-33.190	-383.780	-364.150
158	218	-0.018	-0.001	-0.202	-0.01	0.001	0.022	0.007	0.242	-40.790	-39.290	-447.640	-431.150
179	219	-0.013	0	-0.138	-0	0.001	0.016	0.008	0.178	-45.090	-44.120	-494.740	-484.180
200	220	-0.006	0	-0.070	-0	0.016	0.009	0.011	0.100	-43.330	-47.300	-523.280	-519.040
221	221	0	-0.001	-0.007	-0.01	0.016	0.002	0.017	0.017	-44.120	-48.610	-533.470	-533.470
242	222	0.004	-0.001	0.047	-0.02	0.002	-0.010	0.022	-0.060	-48.080	-48.060	-527.600	-527.320
263	223	0.009	-0.002	0.099	-0.02	0.002	-0.010	0.024	-0.130	-46.250	-45.780	-507.520	-502.400
284	224	0.014	-0.003	0.156	-0.03	0.002	-0.020	0.020	-0.200	-43.070	-41.970	-472.630	-460.600
305	225	0.020	-0.004	0.219	-0.04	0.001	-0.020	0.012	-0.260	-38.360	-36.750	-422.950	-403.220
326	226	0.025	-0.004	0.277	-0.04	0	-0.030	0.004	-0.310	-32.090	-30.250	-352.130	-331.950
347	227	0.029	-0.003	0.316	-0.04	0	-0.030	-0.003	-0.340	-24.540	-22.810	-269.320	-250.350
368	228	0.029	-0.003	0.323	-0.03	-0.001	-0.030	-0.006	-0.340	-16.350	-15.020	-179.450	-164.850
389	229	0.026	-0.002	0.282	-0.02	0	-0.030	-0.005	-0.290	-8.533	-7.773	-93.632	-85.291
410	230	0.016	-0.001	0.178	-0.01	0	-0.020	-0.001	-0.180	-2.506	-2.272	-27.494	-24.925
430	231	0	0	0	0	0	0	0	0	0	0	0	0

*indicate values for the pitted case

Table 4: Maximum values of critical parameters for panel c

Node No.	Response parameter	Max. value
368	θ_x(rad)	0.029
368	θ_x^*(rad)	0.323
215	θ_y(rad)	0.028
215	θ_y^*(rad)	0.312
221	w(mm)	48.614
221	w*(mm)	533.465
14	M_x(KNm)	0.264
14	M_x^*(KNm)	0.264
273	M_y(KNm)	0.468
273	M_y^*(KNm)	0.468

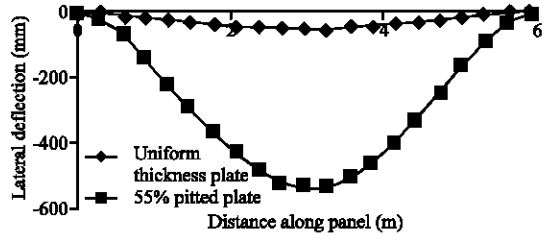

Fig. 7: Longitudinal lateral deflection profile of panel C

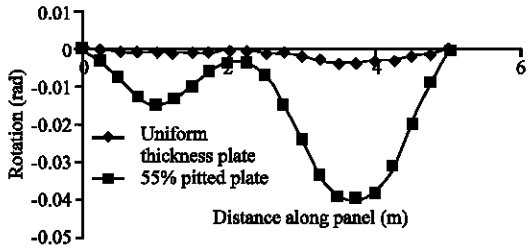

Fig. 8: Longitudinal angular deflection profile of panel C about x

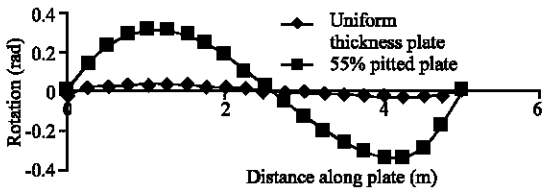

Fig. 9: Longitudinal angular deflection profile of panel C about y

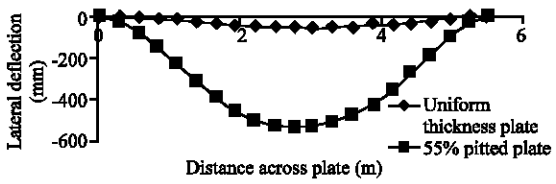

Fig. 10: Transverse lateral deflection profile of panel C

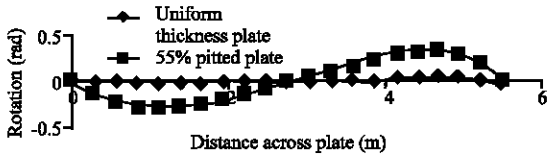

Fig. 11: Transverse angular deflection profile of panel C about x

however, its response even as pitting progressively worsened, stabilized to nearly the same values in both cases.

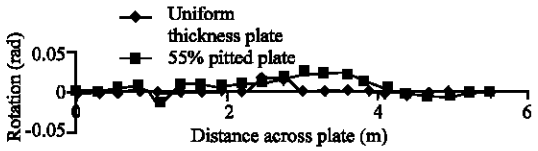

Fig. 12: Transverse angular deflection profile of panel C about y

CONCLUSION

Following the results obtained, it can be generally observed that;

For the isolated analysis of panel A, the simulated load condition resulted in central lateral displacement of 12.492 mm from 5.27 mm observed in the uncorroded case. Maximum deflection after 25% pitting increased correspondingly by 137% to 12.708 mm. A wider margin of increase was similarly observed in the 55% pitted case. From the foregoing, the finite element analysis of the ship deck under consideration revealed that arbitrary thickness losses due to severe pitting have a significant influence on the structural stability and integrity of plates. Maximum allowable displacements increase with increased loss of thickness due to pitting and are more evident as the size of the member and the pitting levels are increased.

Periodic thickness gauging as a corollary of the above is advised in evaluating the structural responses to arbitrary loss of thickness at any time in the service life of the plate, since overstress and consequent failure may result if loading is carried on as initial design specifications allow for such plates.

To improve the versatility of the analytical technique presented in this study, the algorithm can be run by employing 2D and/or 3D elements, which have more elemental nodes and better bending qualities to increase the accuracy of the software.

The concept of variable thickness resulting from corrosion in service and the statistical approach to analyzing pitting profiles of plates presented in this paper can be similarly extended to plates of complex geometries, shells and other structural elements.

Notation:

a,b	=	Plate dimension
x, y	=	Nodal coordinates
M_x, M_y, M_{xy}	=	Moment per unit length
q	=	Load distribution
E	=	Elastic tensile modulus
ν	=	Poisson's ratio
t_0, t, t_e	=	Original, measured and equivalent element plate thicknesses, respectively.
w	=	Deflection
θ_x, θ_y	=	Rotations about x and y axes
$\{\delta^e\}$, $\{\delta\}$	=	Element and structural displacement vectors, respectively
$\{F^e\}$, $\{F\}$	=	Element and structural force vectors respectively
$[K^e]$,[K]	=	Element and overall structural stiffness matrices, respectively

REFERENCES

Akpan, E.R., 2003. Acidic Precipitation and Infrastructural Deterioration in Oil Producing Communities of Akwa Ibom State: A case Study of Eket, South Eastern Nigeria. Global J. Environ. Sci., 2: 47-52.

Bureau Veritas Marine Division, 2000. Rules For The Classification of Steel Ships, Part A-Classification and Survey, Bureau Veritas, Paris, France.

Clough, R.W., M.J. Turner, H.C. Martins and L.J. Topp, 1956. Stiffness and Deflection Analysis of Complex Structures. J. Aeronautical Sci., 23: 805-823.

Climate Justice, 2005. Gas Flaring in Nigeria: A Human Rights, Environmental and Economic Monstrosity, A report by the climate Justice Program and Environmental Rights Action/Friends of the Earth Nigeria, http://www.climate law.org/gas.flaring/ report/section7.html.

Corrosion Doctor, 2007. Corrosion Fatigue Models, http://www.corrosion-doctors.org/site-map.htm.

Ibekwe, U.A., 2006. Finite Element Stress Analysis of a Corroded Plate, M. Tech. Thesis, RSUST, Port Harcourt, Nigeria.

Johnary, T.N., 2005. Safety and Structural Assemblages: Cascading Frontiers, Inaugural Lecture Series. Rivers State University of Science and Technology, Port Harcourt, Nigeria, 14: 71-74.

Lakhote, R.V., M.D. Pandey and A.N. Sherbourne, 2002. Buckling Behaviour of Corroded Plates, http://www.ce.utexas.edu/em2000/papers/RVLakhot e.pdf.

Lloyd's Register, 1997. Classification of Ships-Rules and Regulations Part 2-Manufacturing, Testing and Certification of Materials.

Rockey, K.C., H.R. Evans, D.W. Griffiths and D.A. Nethercot, 1973. The Finite Element Method, A Basic Introduction. 2nd Edn. John Wiley and Sons, New York.

Roorda, J., N.K. Srivastava, A. Maslouhi and A.N. Sherbourne, 1996. Residual Strength of Ship Structures With Corrosion-Induced Damage. A Report to the Defence Research Establishment, Atlantic Halifax, Canada.

Ross, C.T.F., 1982. Computational Methods in Stress Analysis. Ellis Hoodwood, Chichester, UK.

Sletten, R. and B. Pedersen, 1974. Application of the Finite Element Method to Offshore Structures. Computer and Structures, 4: 131-148.

Timoshenko, S. and S.E. Woinowsky-Krieger, 1959. Theory of Plates and Shells. 2nd Edn. McGraw Hill, New York.

Zienkiewicz, O.C., 1971. The Finite Element Method. McGraw-Hill, New York.